Supplementary material

Copper(I) ionic complexes based on imidazo[4,5-f][1,10]phenanthrolin diimine chelating ligands: crystal structures, photo- and electroluminescent properties.

Anton V. Rozhkov,[a]* Svetlana N. Eliseeva,[a] Sergey V. Baykov,[a] Lev E. Zelenkov,[a] Dmitry O. Goriachiy,[b] and Ilya V. Taydakov[b]

[a]Institute of Chemistry, Saint Petersburg State University, Universitetskaya Nab. 7/9, 199034 Saint Petersburg, Russian Federation.

[b]P.N. Lebedev Physical Institute of the Russian Academy of Science, Leninsky pr., 53, 119991 Moscow, Russian Federation.

*Corresponding author

E-mail: iomcrozhkov@gmail.com

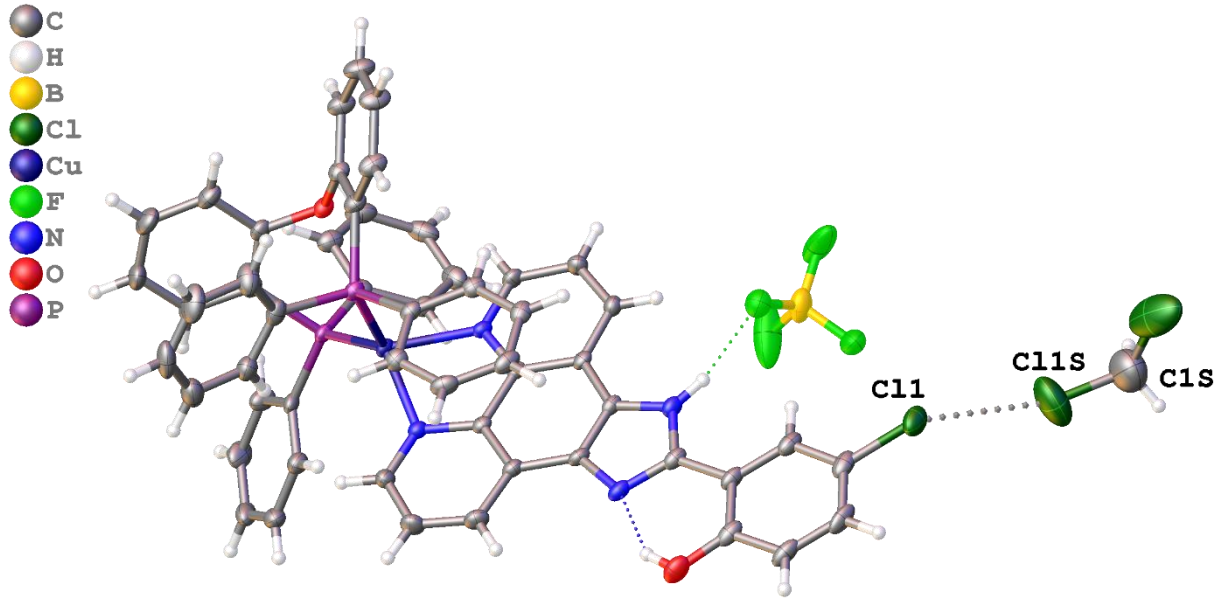

Figure S1. Intermolecular halogen bonding in **2**·CH_2Cl_2.

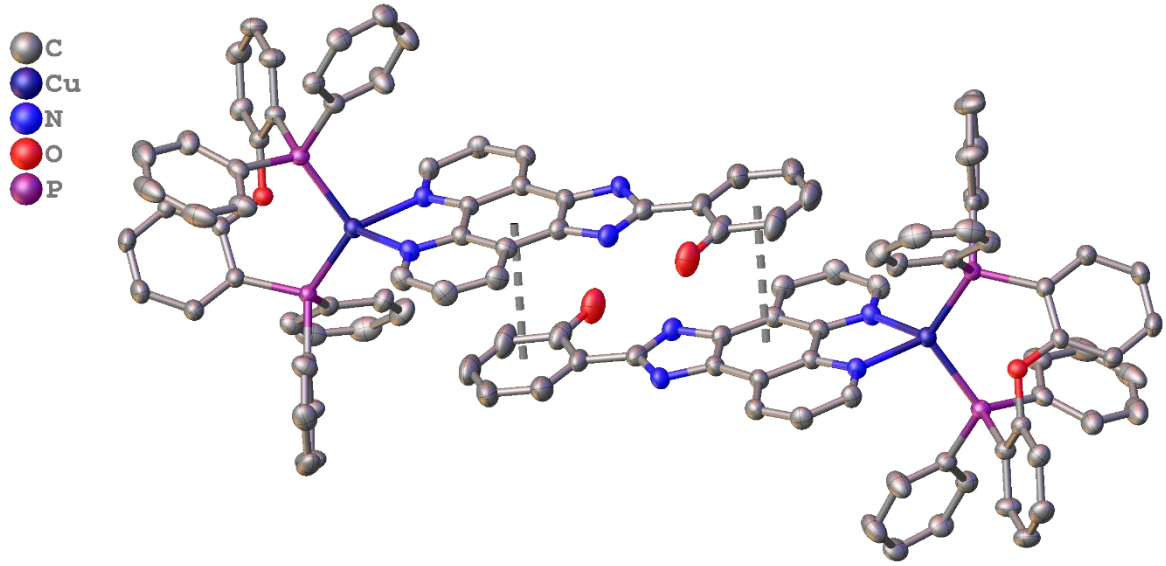

Figure S2. Intramolecular π···π interaction in **1**. Hydrogen atoms are omitted for clarity

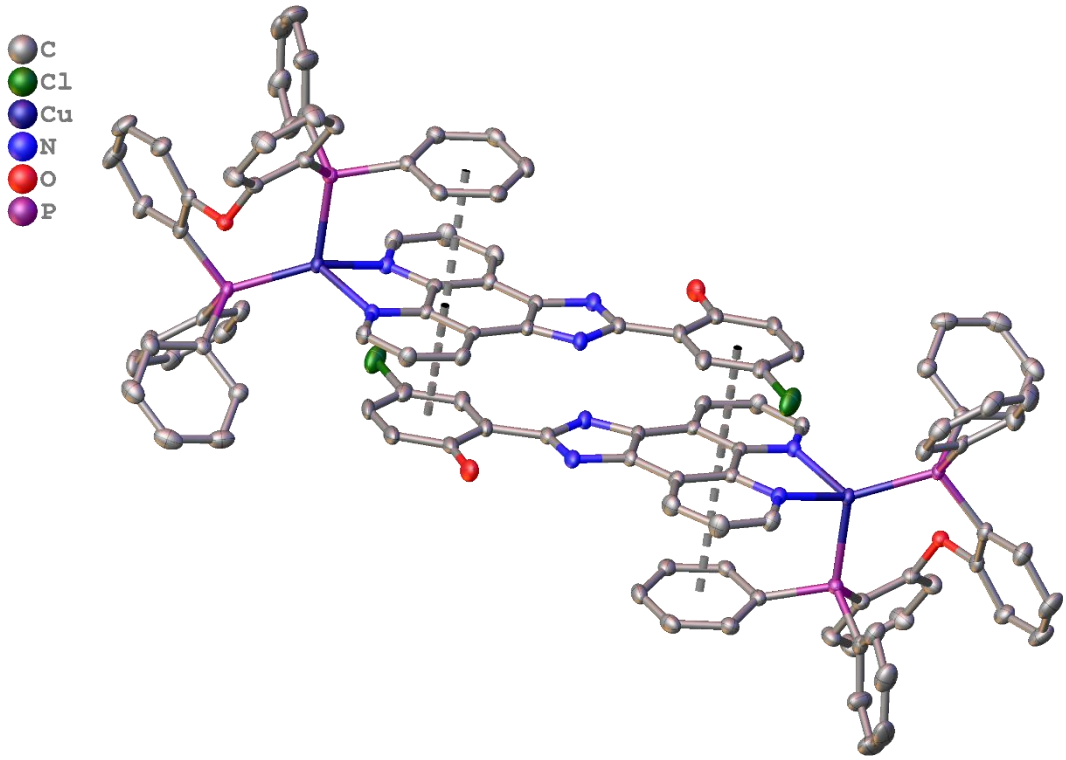

Figure S3. Intra- and intermolecular π···π interaction in **2**. Hydrogen atoms are omitted for clarity.

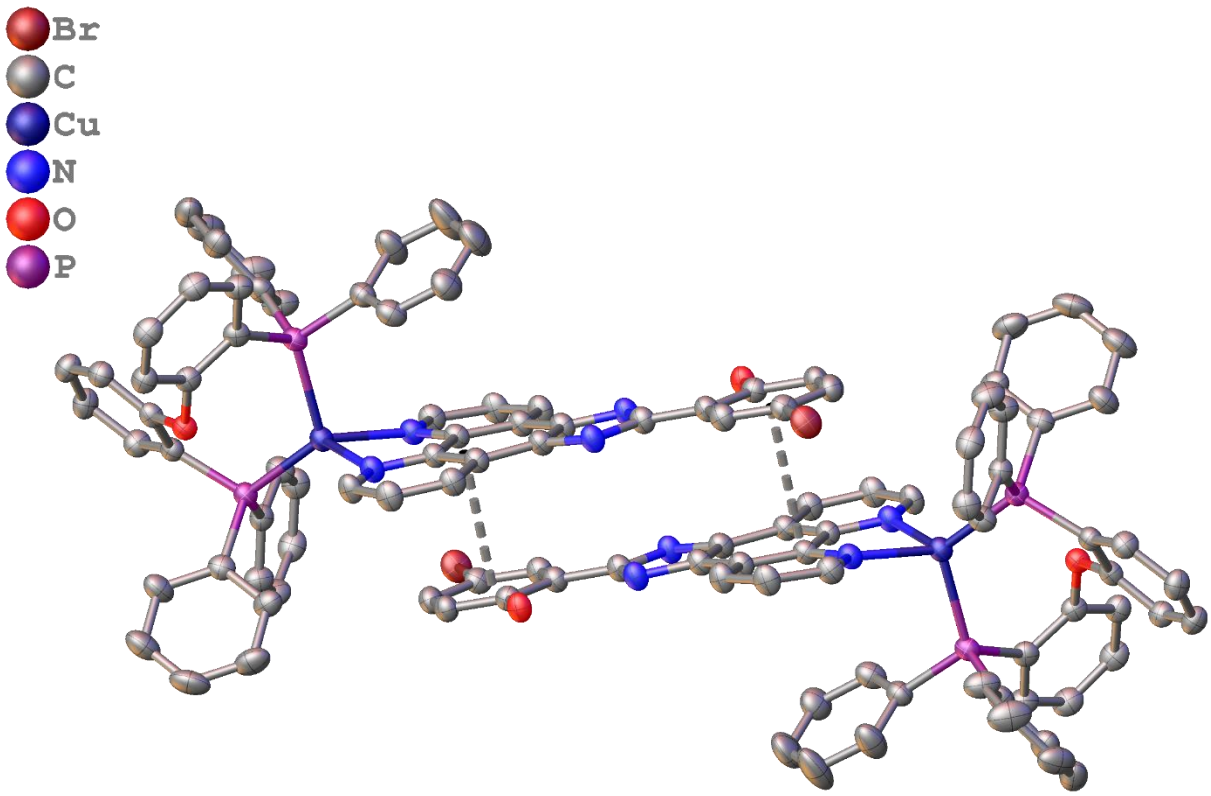

Figure S4. Intermolecular π···π interaction in **3**. Hydrogen atoms are omitted for clarity.

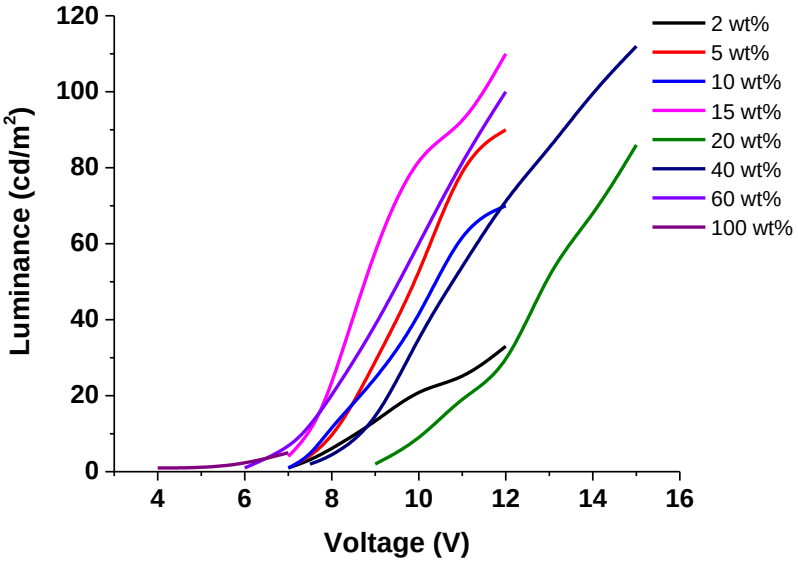

Figure S5. Luminance-voltage curves of device ITO/PEDOT:PSS/**1**:CBP/TPBI/LiF/Al at different host-guest ratio.

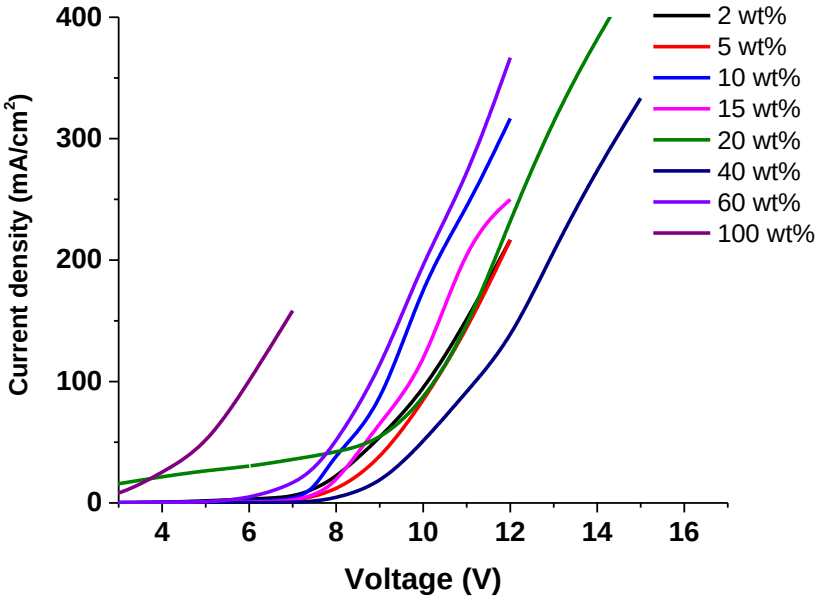

Figure S6. Current density-voltage curves of device ITO/PEDOT:PSS/**1**:CBP/TPBI/LiF/Al at different host-guest ratio.

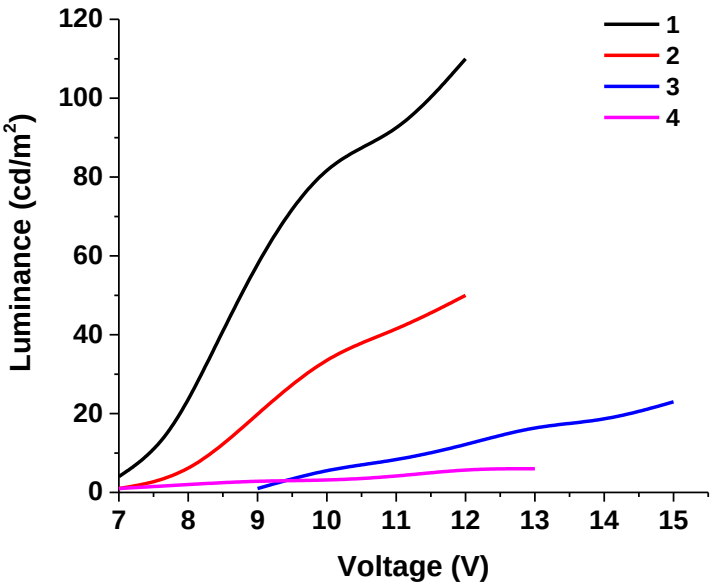

Figure S7. Luminance-voltage curves of device ITO/PEDOT:PSS/**complex**:CBP (15% wt.)/TPBI/LiF/Al.

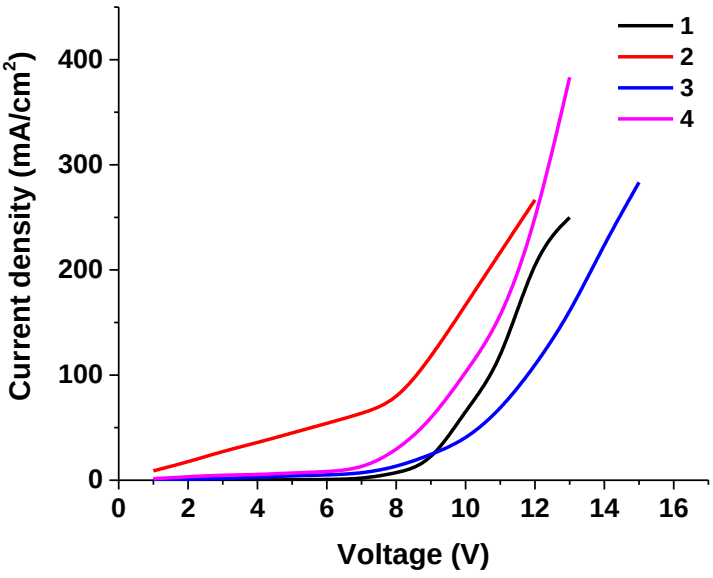

Figure S8. Current density-voltage curves of device ITO/PEDOT:PSS/**complex**:CBP (15% wt.)/TPBI/LiF/Al.

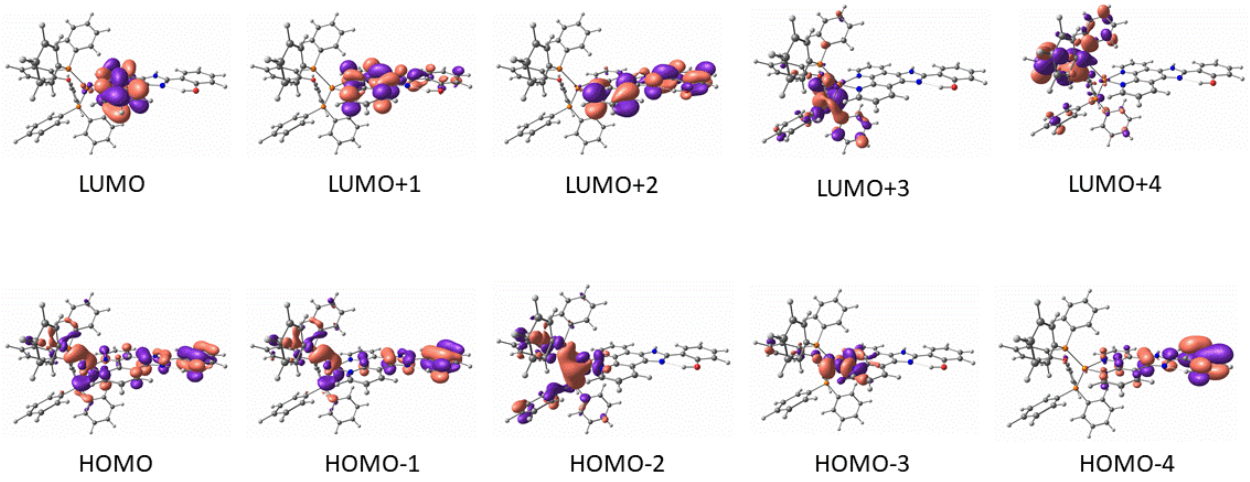

Figure S9. Frontier orbitals of **1**.

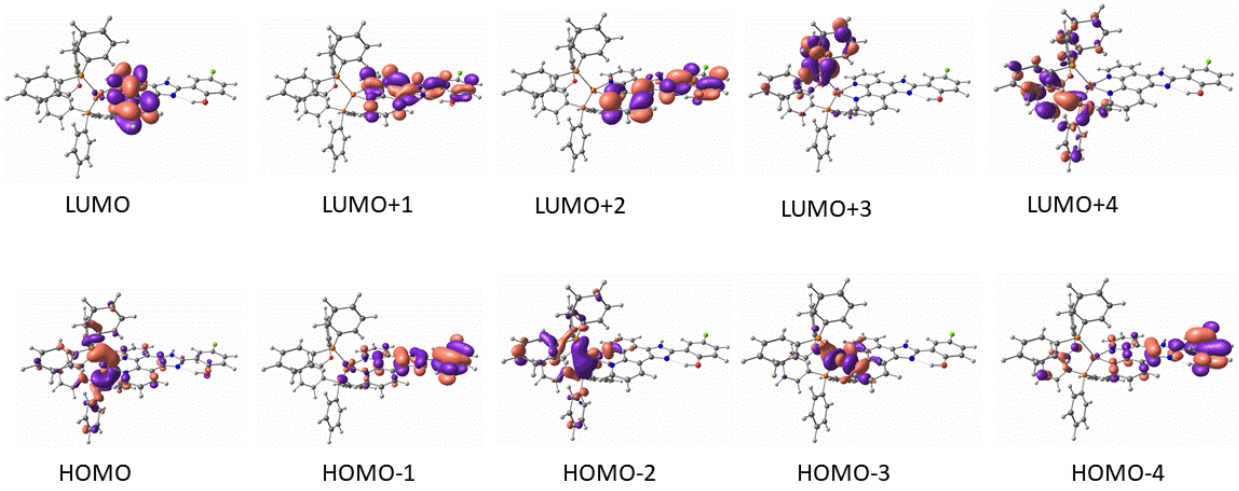

Figure S10. Frontier orbitals of **2**.

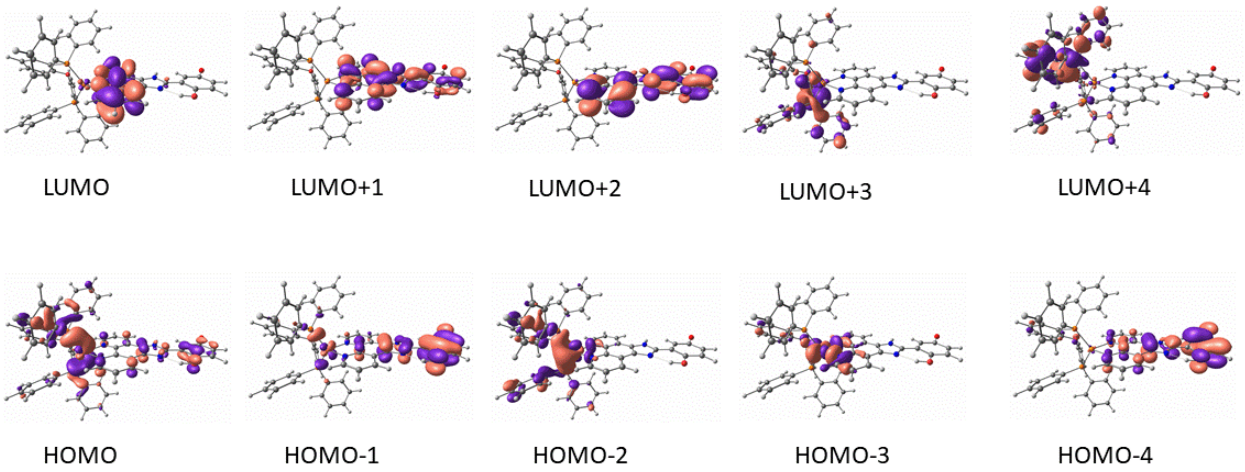

Figure S11. Frontier orbitals of **3**.

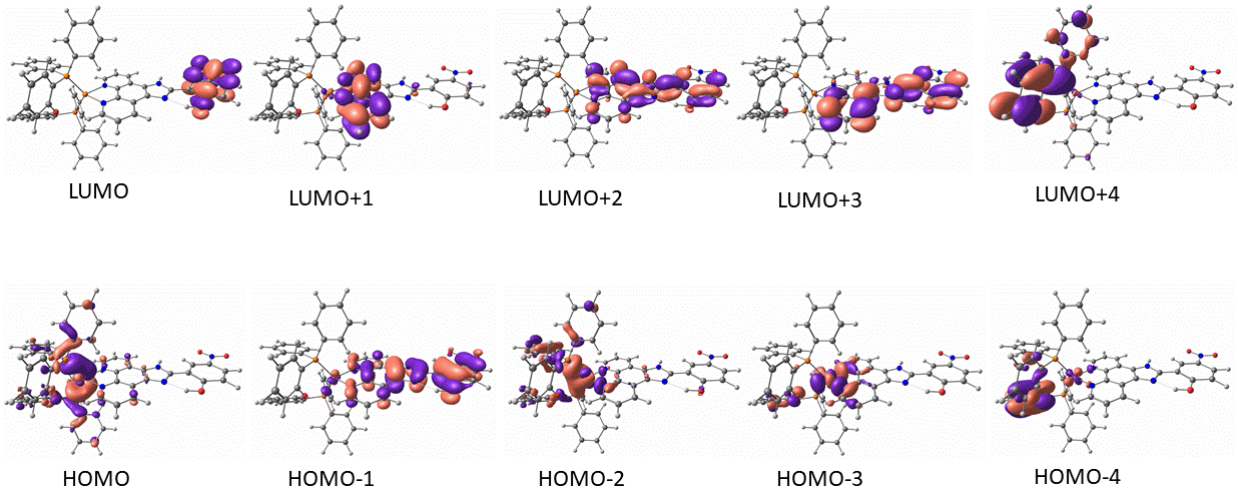

Figure S12. Frontier orbitals of **4**.

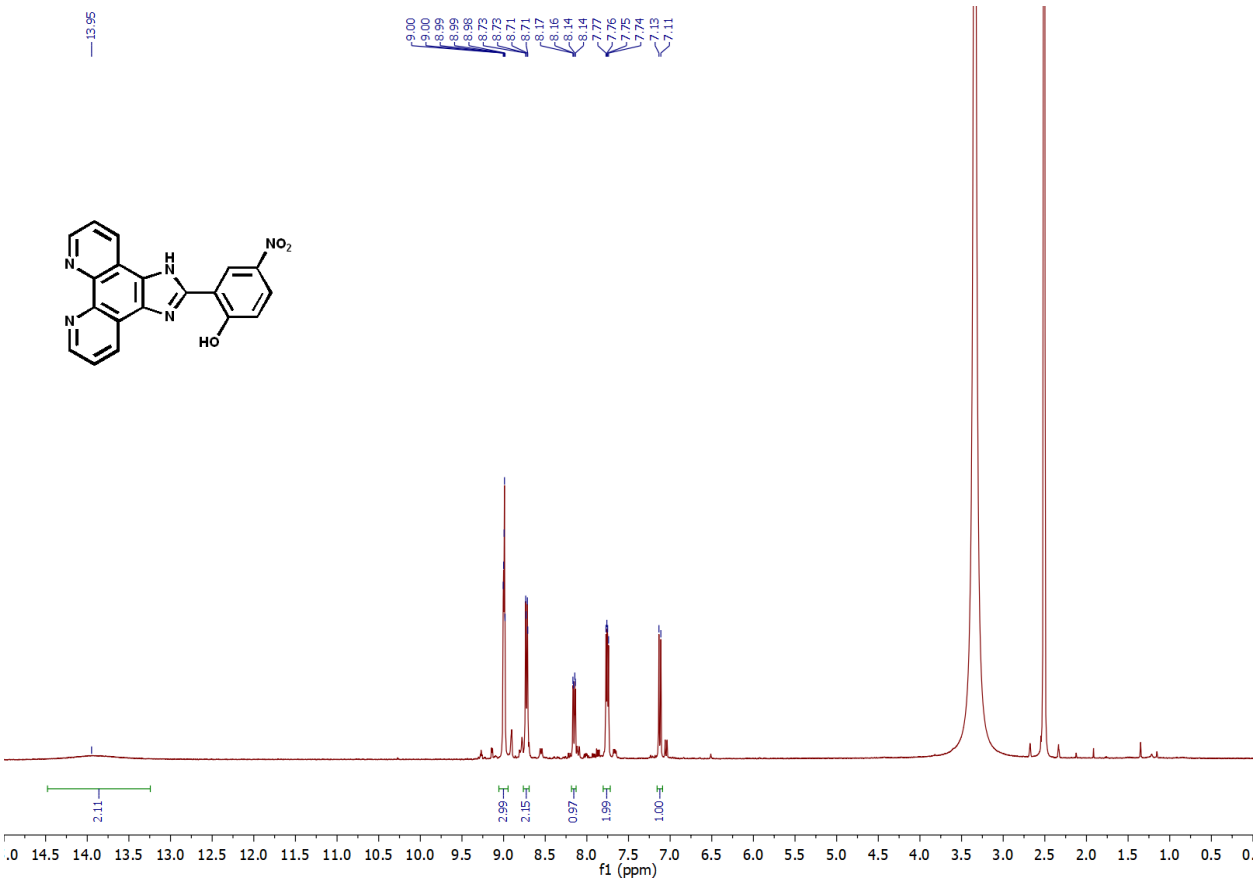

Figure S13. ^{1}H NMR spectrum of **L4**.

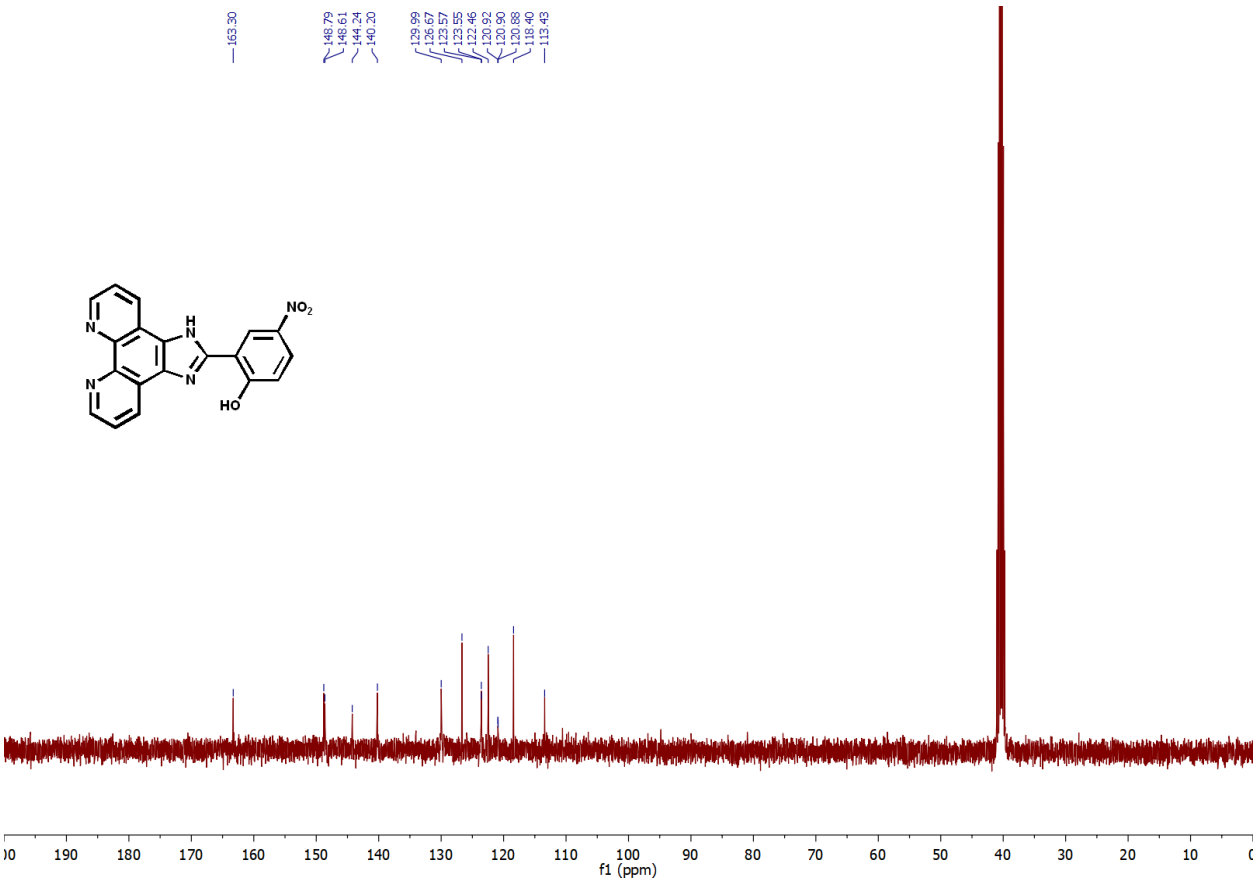

Figure S14. ^{13}C NMR spectrum of **L4**.

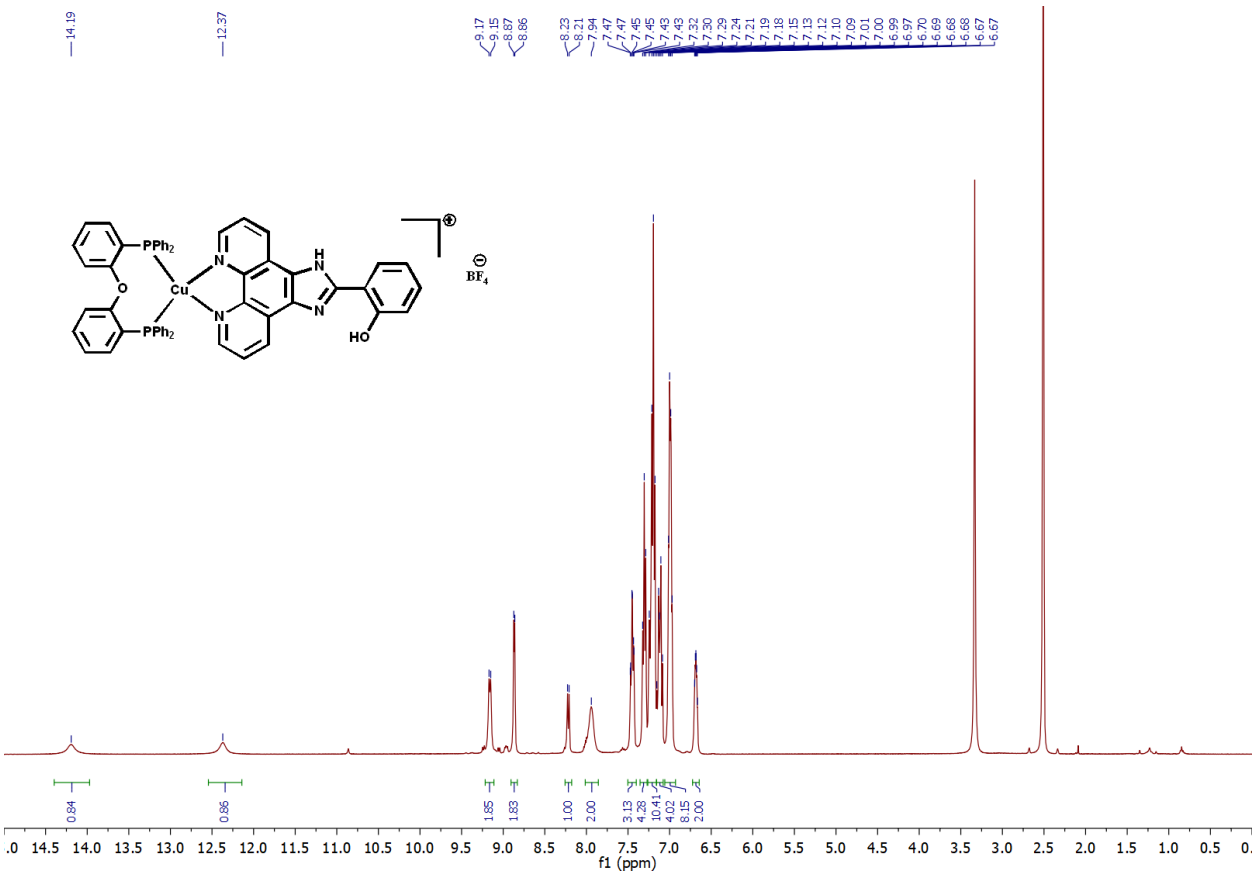

Figure S15. ^{1}H NMR spectrum of **1**.

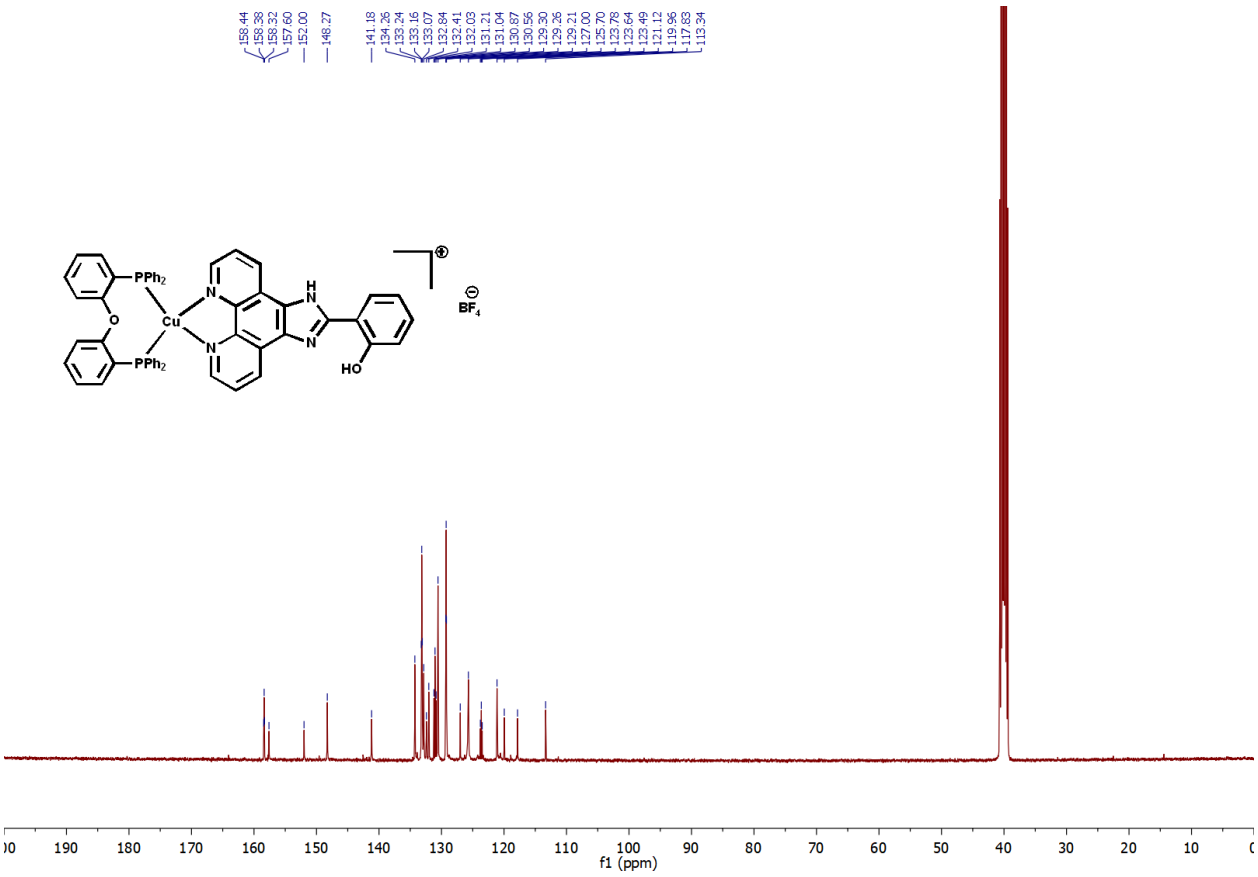

Figure S16. ^{13}C NMR spectrum of **1**.

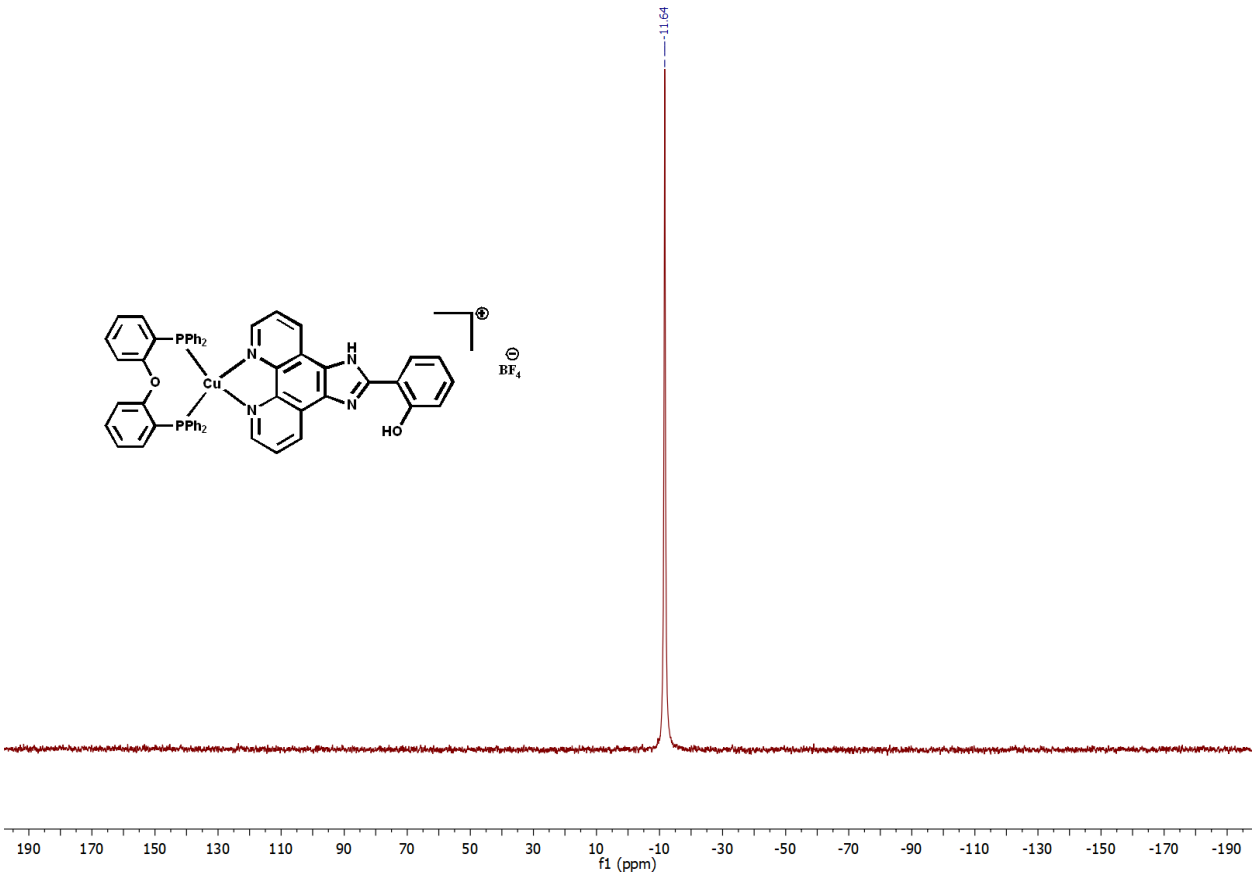

Figure S17. ^{31}P NMR spectrum of **1**.

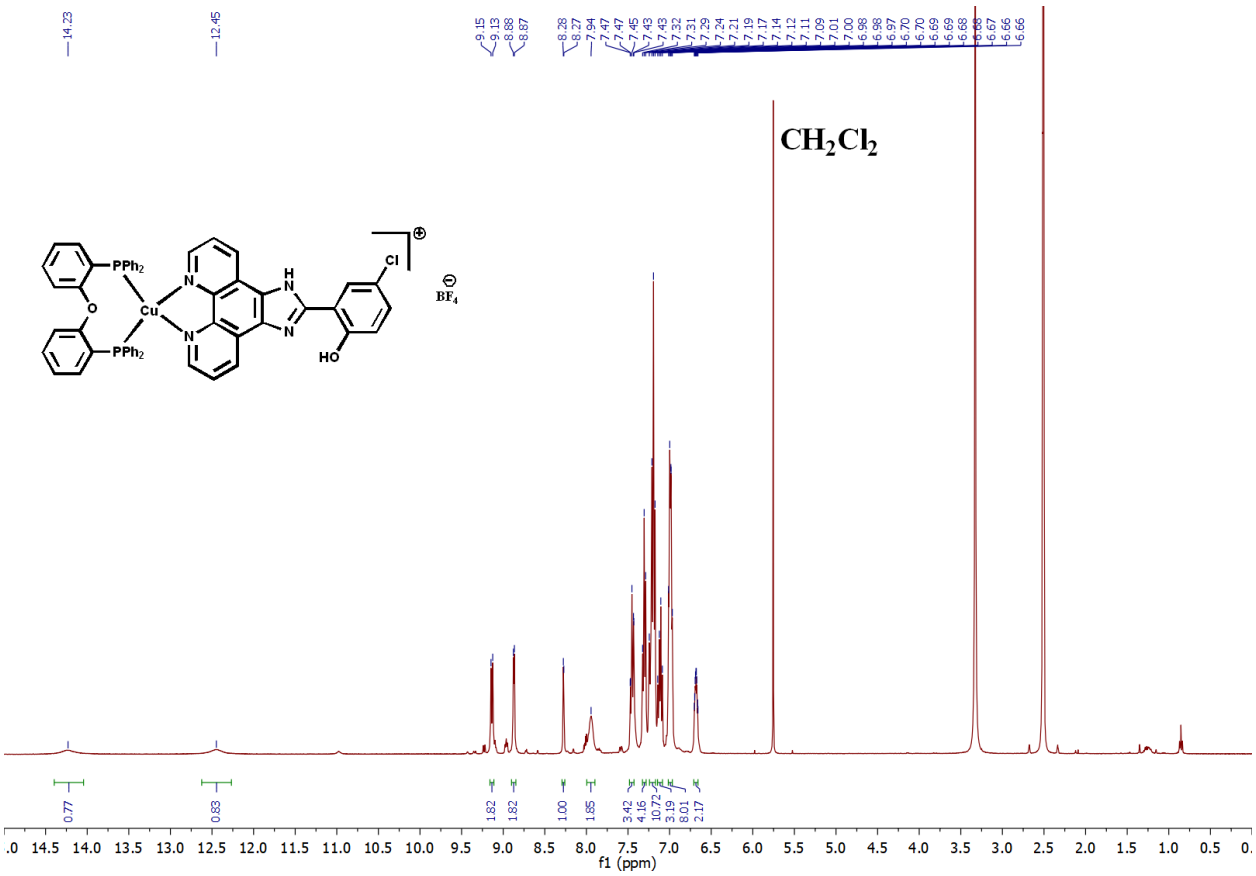

Figure S18. ^{1}H NMR spectrum of **2**.

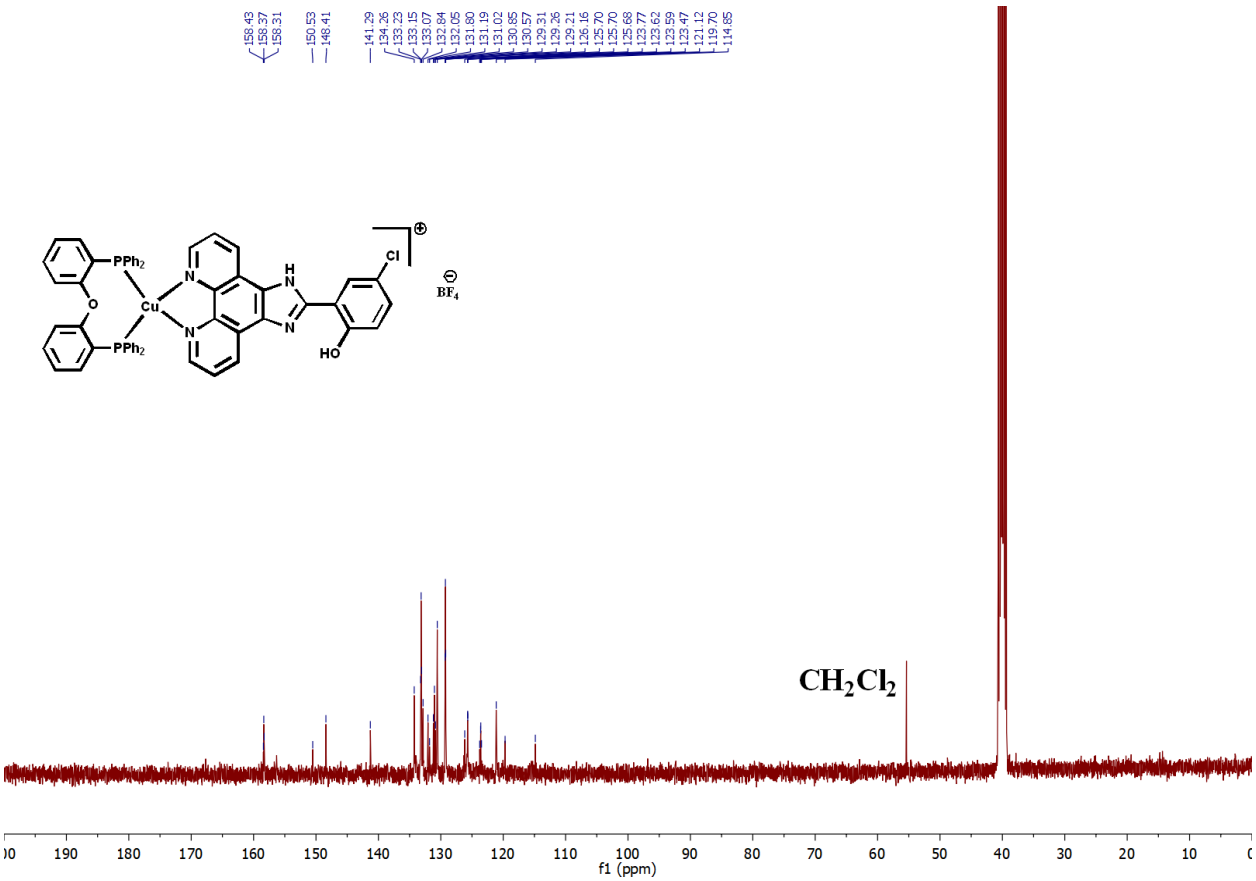

Figure S19. ^{13}C NMR spectrum of **2**.

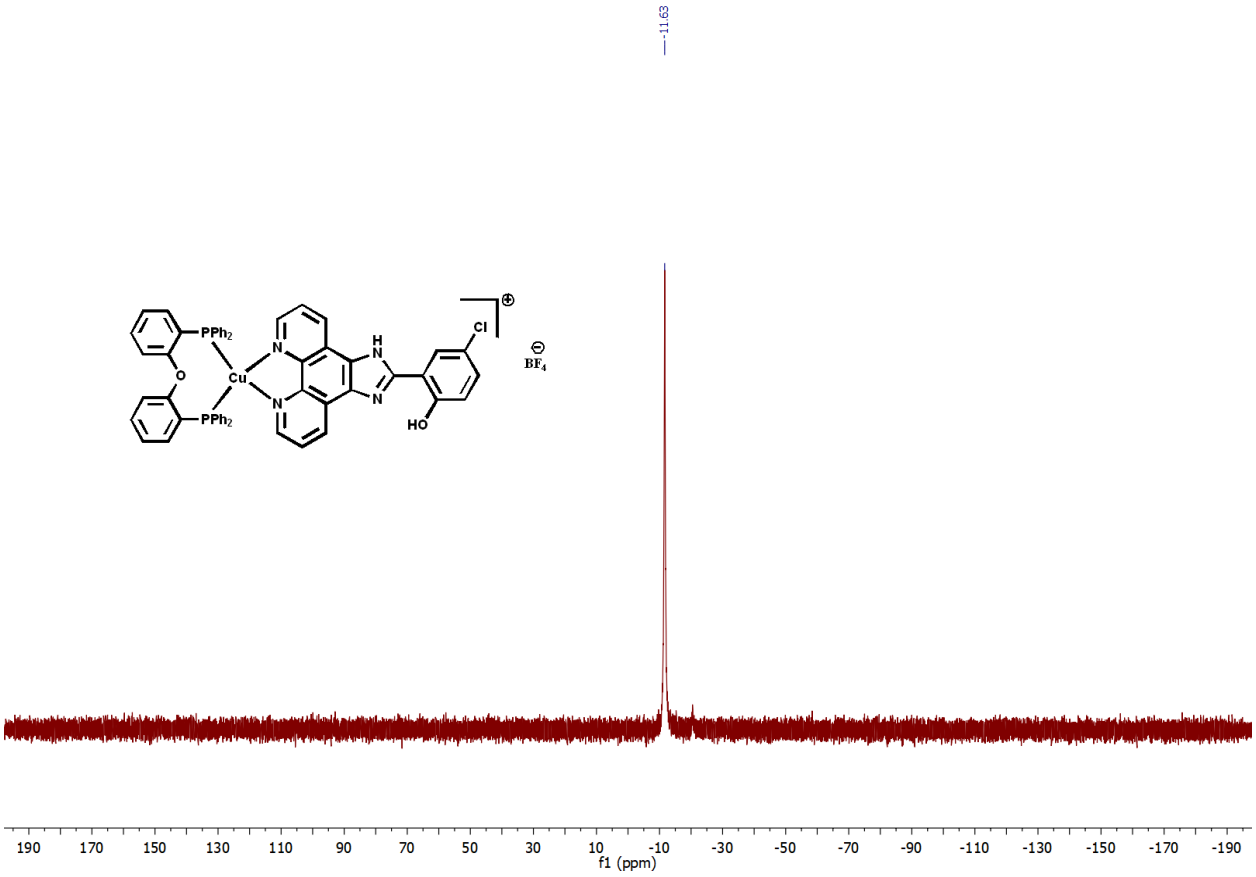

Figure S20. ^{31}P NMR spectrum of **2**.

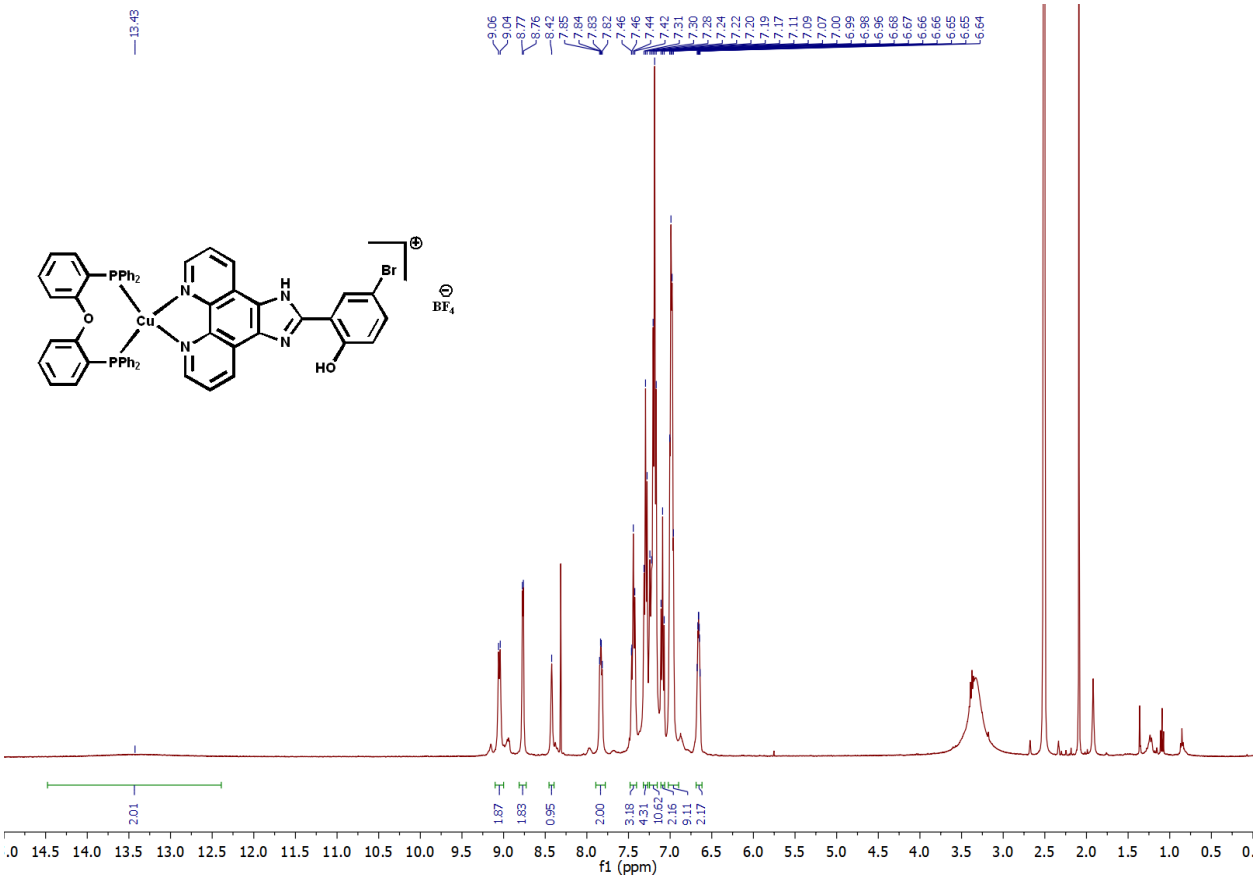

Figure S21. ^{1}H NMR spectrum of **3**.

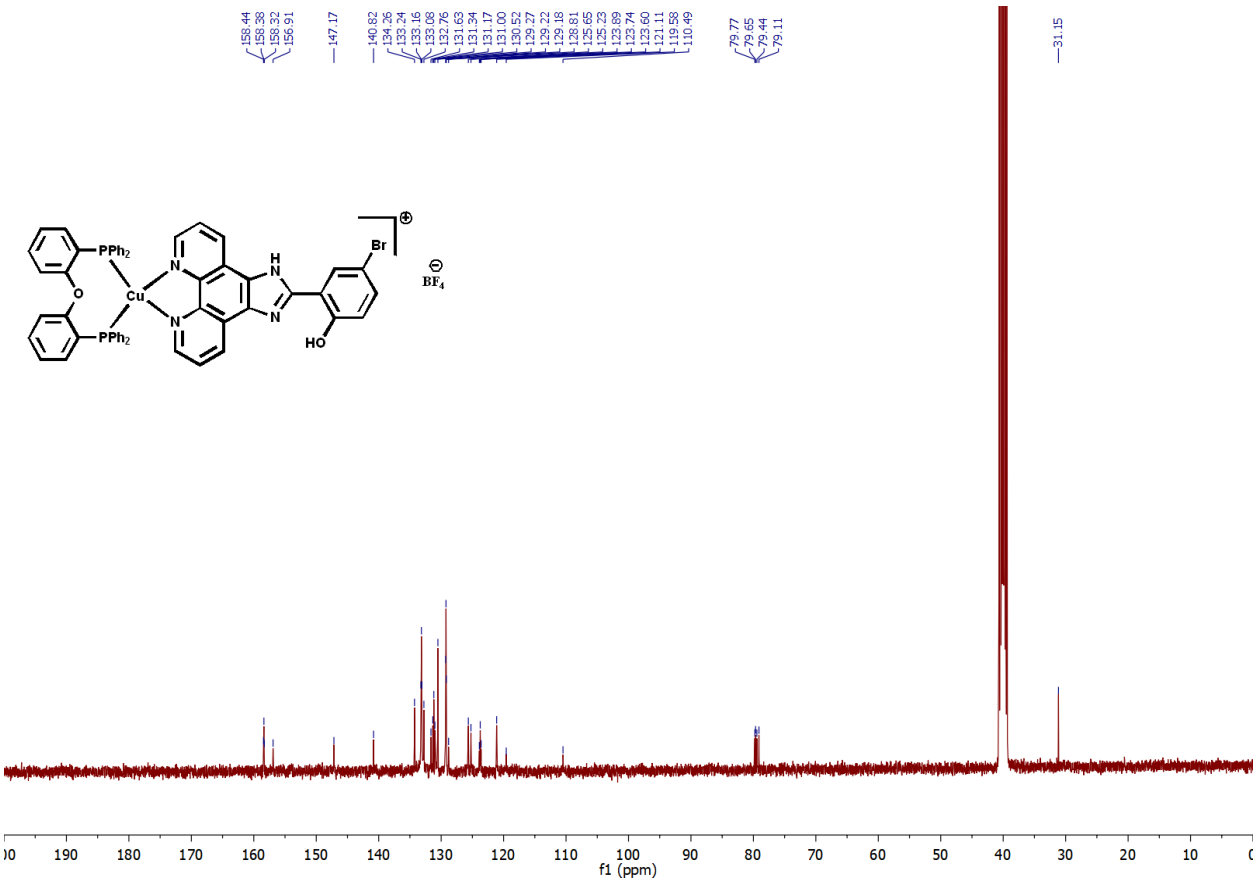

Figure S22. ^{13}C NMR spectrum of **3**.

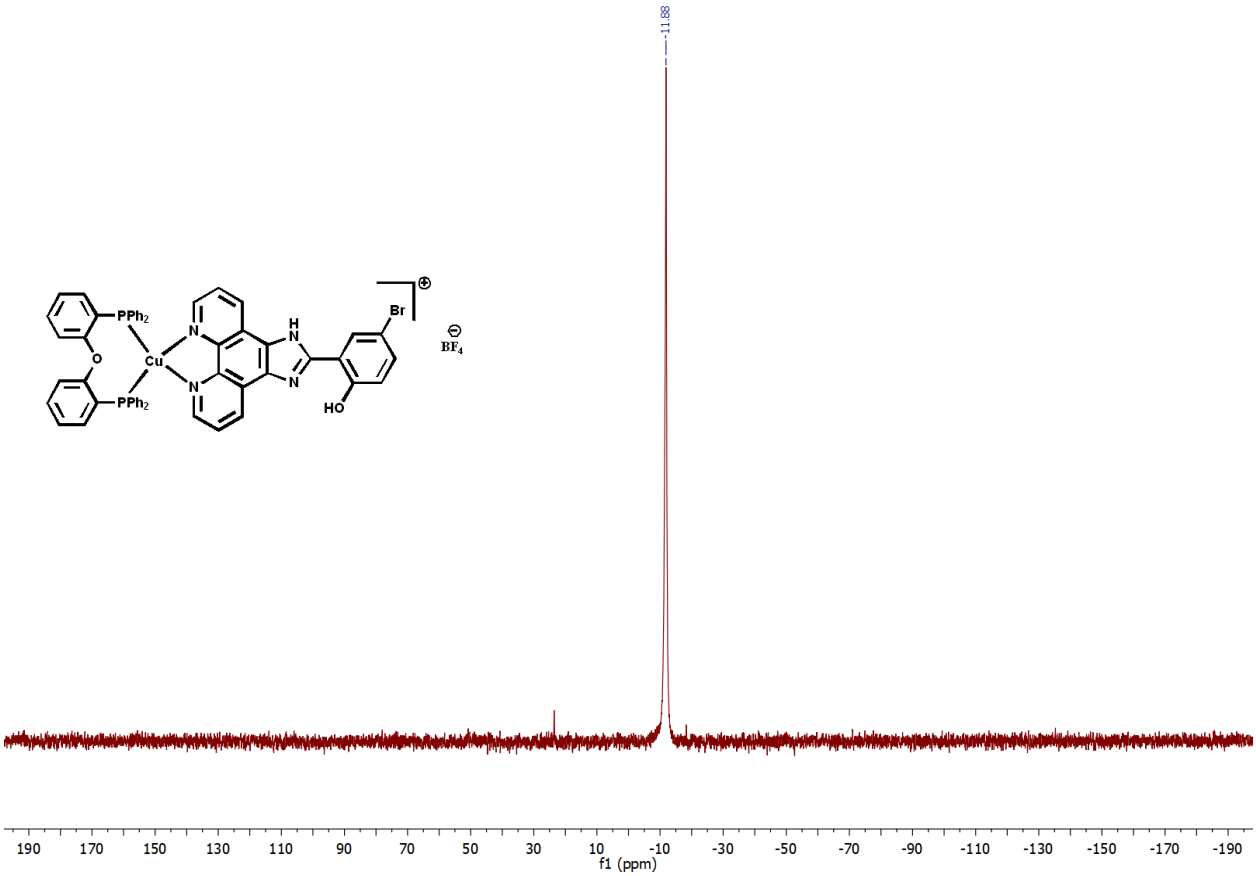

Figure S23. ^{31}P NMR spectrum of **3**.

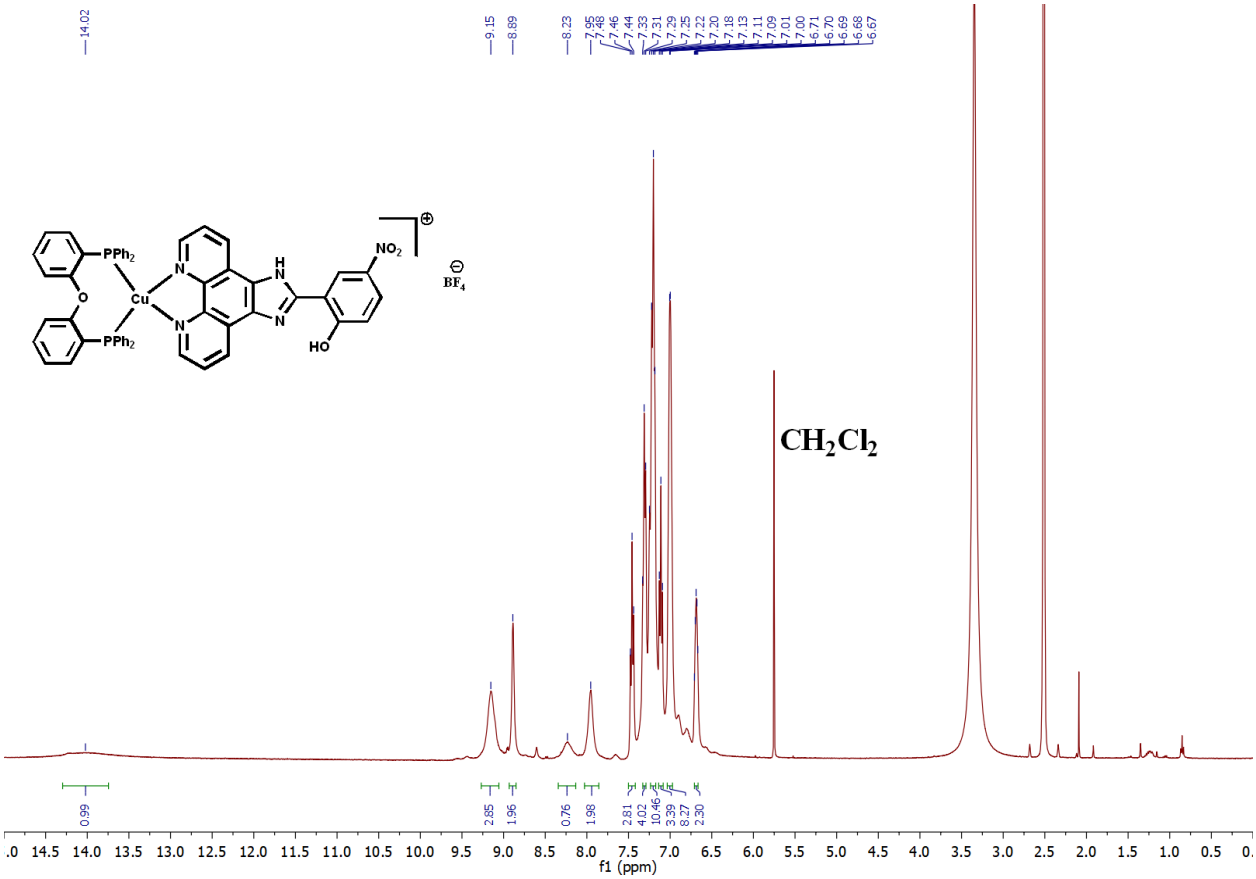

Figure S24. ^{1}H NMR spectrum of **4**.

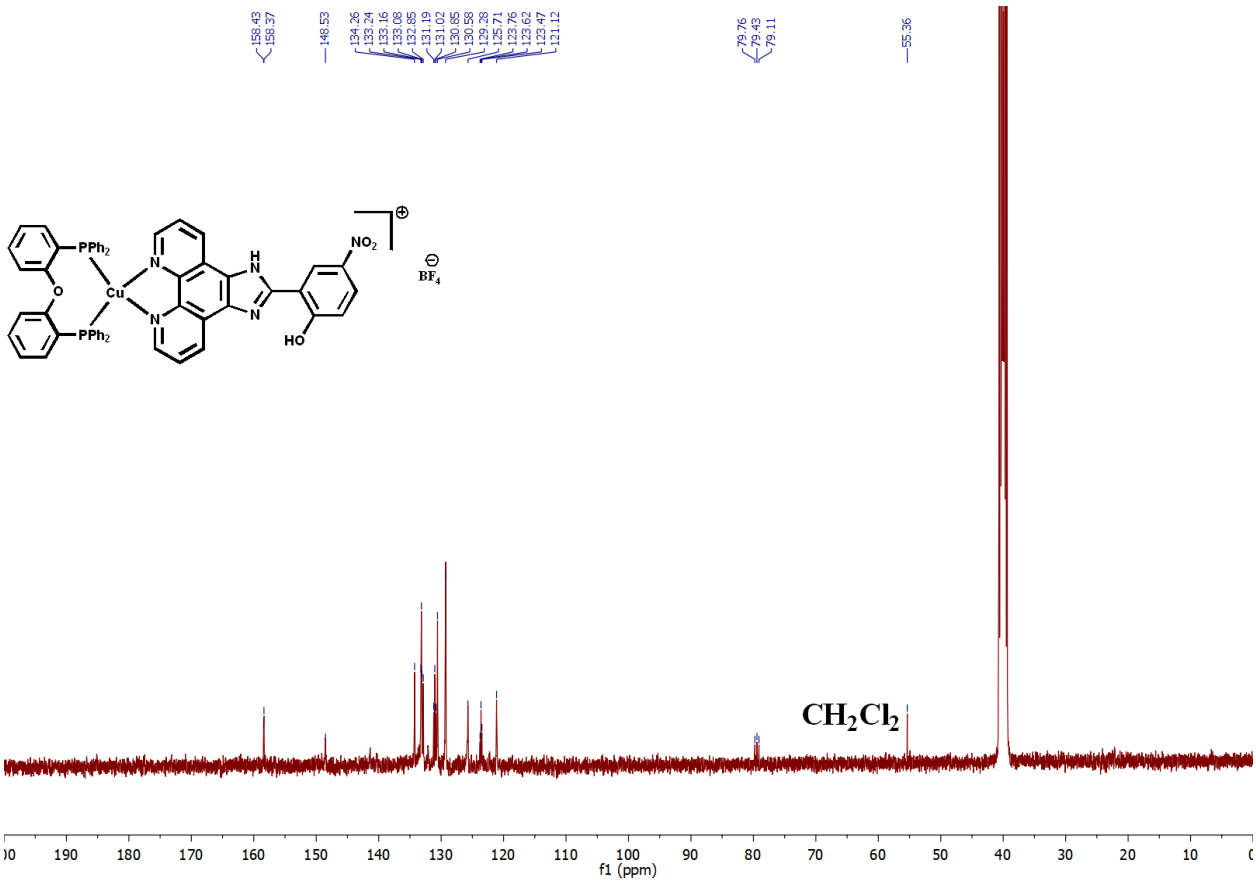

Figure S25. ^{13}C NMR spectrum of **4**.

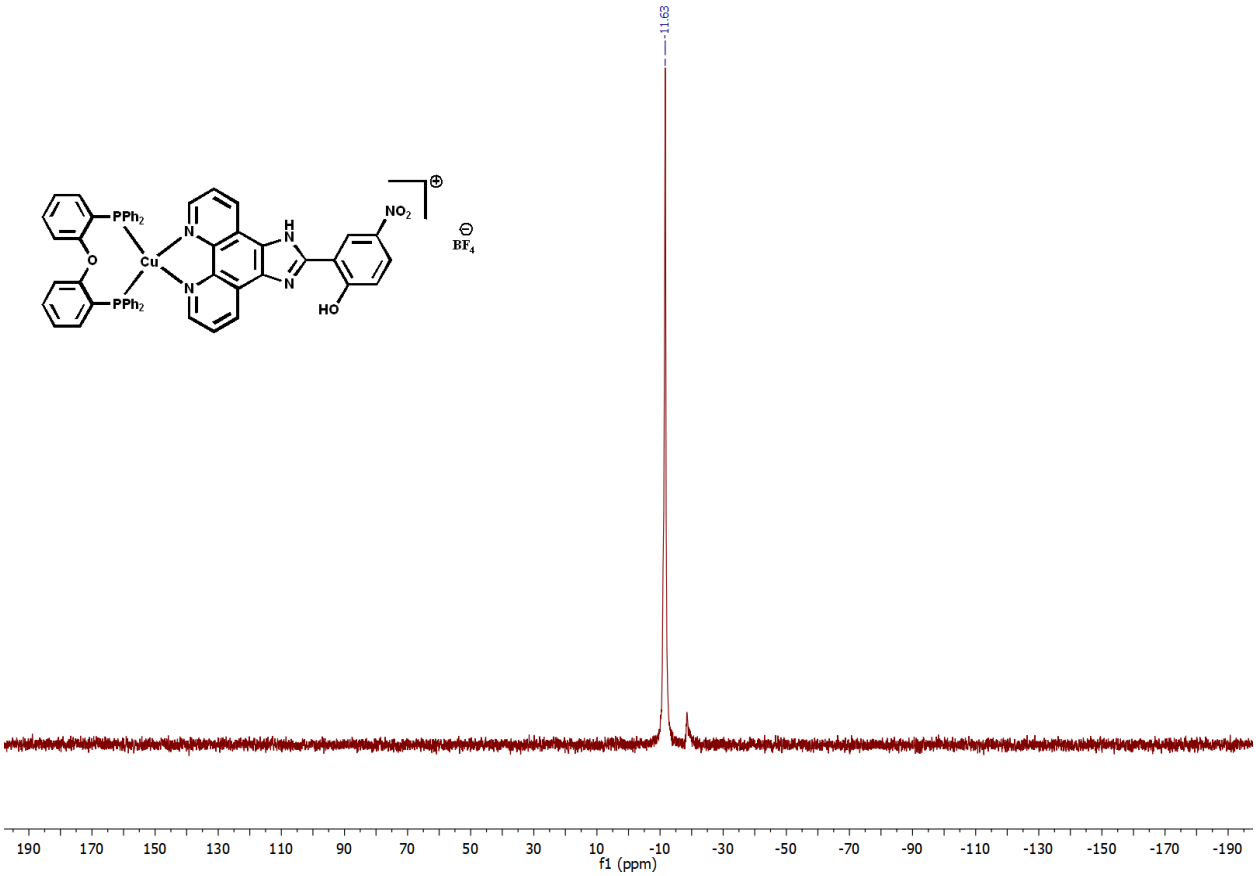

Figure S26. ^{31}P NMR spectrum of **4**.

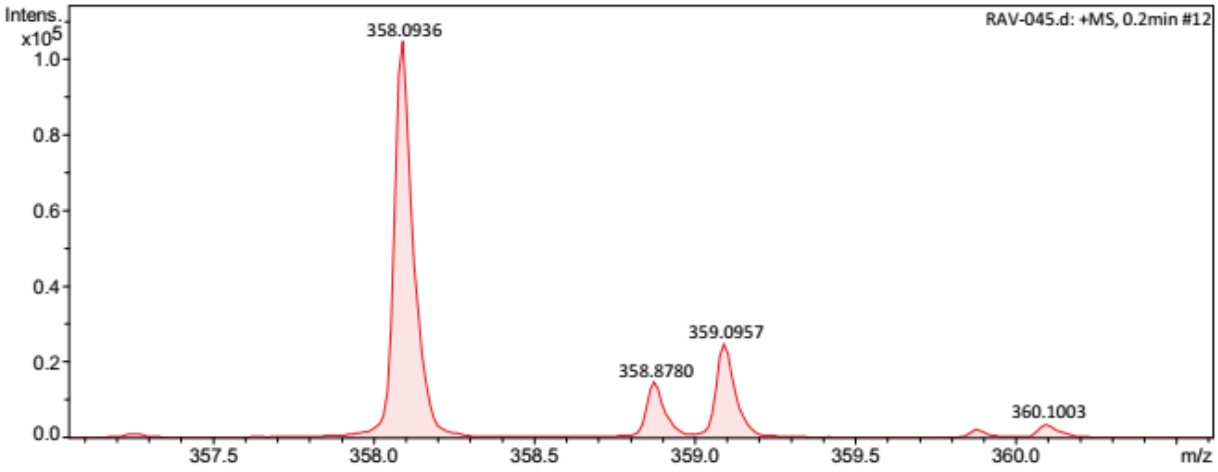

Figure S27. HRESI-MS spectrum of **L4**.

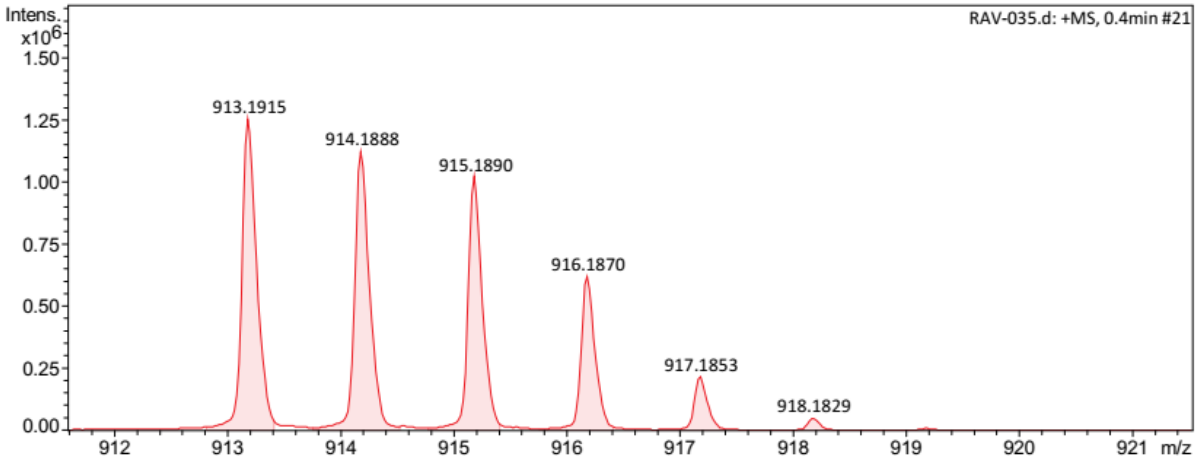

Figure S28. HRESI-MS spectrum of **1**.

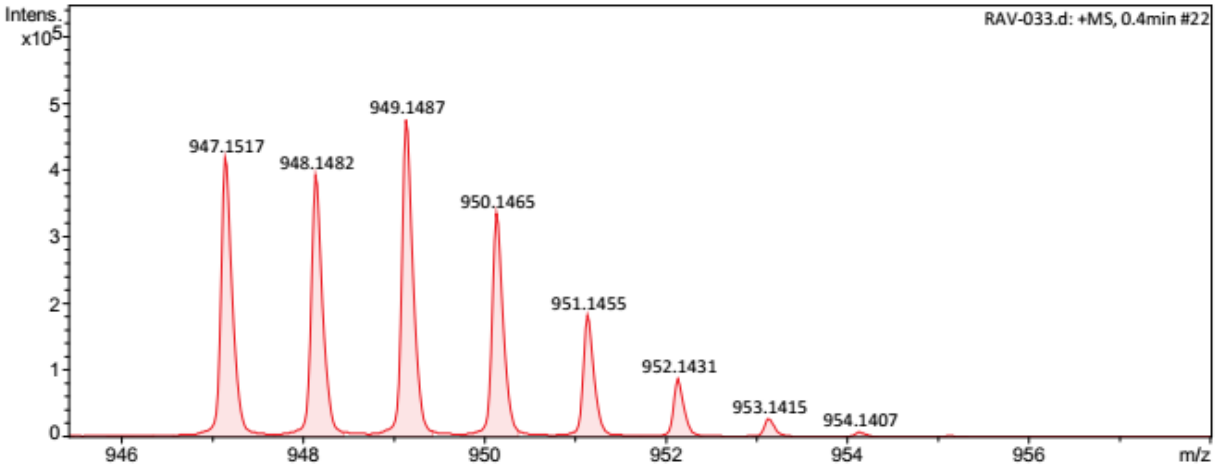

Figure S29. HRESI-MS spectrum of **2**.

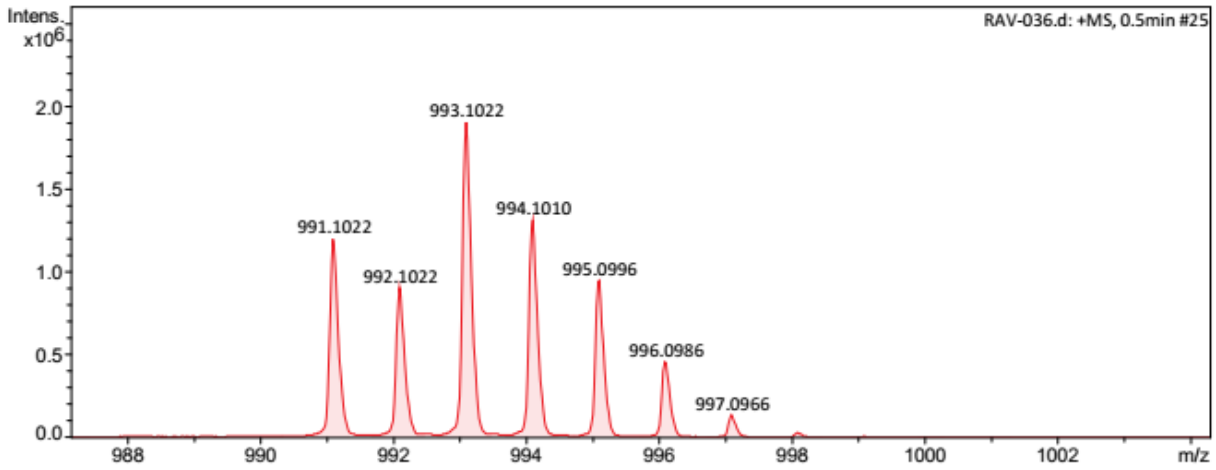

Figure S30. HRESI-MS spectrum of **3**.

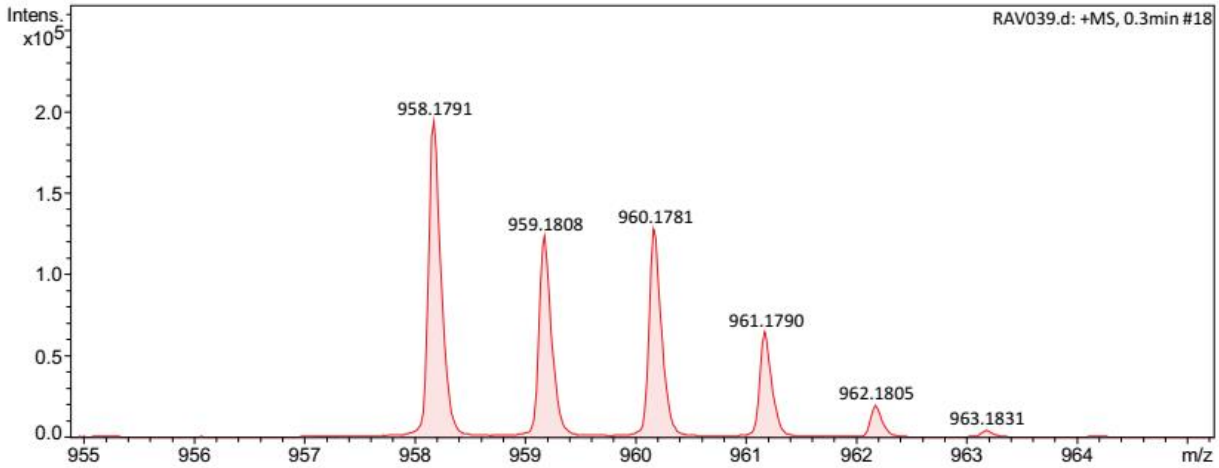

Figure S31. ESI-MS spectrum of **4**.

Table S1. Crystal data and structure refinement parameters for **1**, **2,** and **3**.

	1	**2**	**3**
Empirical formula	$C_{57}H_{46}BCuF_4N_4O_3P_2S$	$C_{56}H_{41}BCl_3CuF_4N_4O_2P_2$	$C_{55}H_{39}BBrCuF_4N_4O_2P_2$
Formula weight	1079.33	1120.57	1080.10
Temperature/K	130.0(2)	100	99.9(5)
Crystal system	monoclinic	monoclinic	triclinic
Space group	$P2_1/n$	$P2_1/c$	P-1
a/Å	17.63140(10)	17.4377(5)	13.1619(3)
b/Å	16.24840(10)	15.4971(3)	14.2651(2)

c/Å	17.9278(2)	20.1990(5)	14.9940(3)
α/°	90	90	100.1100(10)
β/°	90.9260(10)	94.279(2)	103.415(2)
γ/°	90	90	111.011(2)
Volume/Å^3	5135.32(7)	5443.2(2)	2450.37(9)
Z	4	4	2
ρ_{calc}g/cm^3	1.396	1.367	1.464
μ/mm^{-1}	2.102	0.666	2.721
F(000)	2224.0	2288.0	1096.0
Crystal size/mm^3	0.13 × 0.12 × 0.11	0.21 × 0.18 × 0.16	0.15 × 0.1 × 0.09
Radiation	CuKα (λ = 1.54184)	MoKα (λ = 0.71073)	CuKα (λ = 1.54184)
2Θ range for data collection/°	6.976 to 148.048	5.23 to 54.996	6.322 to 141.154
Index ranges	-21 ≤ h ≤ 21, -20 ≤ k ≤ 20, -22 ≤ l ≤ 21	-22 ≤ h ≤ 22, -20 ≤ k ≤ 19, -26 ≤ l ≤ 24	-14 ≤ h ≤ 16, -17 ≤ k ≤ 15, -18 ≤ l ≤ 18
Reflections collected	65708	43848	40971
Independent reflections	10330 [R_{int} = 0.0355, R_{sigma} = 0.0227]	12469 [R_{int} = 0.0290, R_{sigma} = 0.0310]	9295 [R_{int} = 0.0451, R_{sigma} = 0.0360]
Data/restraints/parameters	10330/0/661	12469/0/659	9295/0/632
Goodness-of-fit on F^2	1.037	1.028	1.079
Final R indexes [I>=2σ (I)]	R_1 = 0.0567, wR_2 = 0.1561	R_1 = 0.0590, wR_2 = 0.1456	R_1 = 0.0455, wR_2 = 0.1213
Final R indexes [all data]	R_1 = 0.0604, wR_2 = 0.1594	R_1 = 0.0762, wR_2 = 0.1616	R_1 = 0.0523, wR_2 = 0.1255
Largest diff. peak/hole / e Å^{-3}	1.24/-1.23	1.52/-1.72	0.91/-0.71